Inorganic Chemistry

ARTICLE

pubs.acs.org/IC

Macrocyclic Receptor Showing Extremely High Sr(II)/Ca(II) and Pb(II)/Ca(II) Selectivities with Potential Application in Chelation Treatment of Metal Intoxication

Raquel Ferreirós-Martínez,[†] David Esteban-Gómez,[†] Éva Tóth,[‡] Andrés de Blas,[†] Carlos Platas-Iglesias,*[,†] and Teresa Rodríguez-Blas*[,†]

[†]Departamento de Química Fundamental, Universidade da Coruña, Campus da Zapateira, Rúa da Fraga 10, 15008 A Coruña, Spain

[‡]Centre de Biophysique Moléculaire, CNRS, Rue Charles Sadron, 45071 Orléans, Cedex 2, France

Supporting Information

ABSTRACT: Herein we report a detailed investigation of the complexation properties of the macrocyclic decadentate receptor *N*,*N*′-Bis[(6-carboxy-2-pyridil)methyl]-4,13-diaza-18-crown-6 (H_2bp18c6) toward different divalent metal ions [Zn(II), Cd(II), Pb(II), Sr(II), and Ca(II)] in aqueous solution. We have found that this ligand is especially suited for the complexation of large metal ions such as Sr(II) and Pb(II), which results in very high Pb(II)/Ca(II) and Pb(II)/Zn(II) selectivities (in fact, higher than those found for ligands widely used for the treatment of lead poisoning such as ethylenediaminetetraacetic acid (edta)), as well as in the highest Sr(II)/Ca(II) selectivity reported so far. These results have been rationalized on the basis of the structure of the complexes. X-ray crystal diffraction, ^{1}H and ^{13}C NMR spectroscopy, as well as theoretical calculations at the density functional theory (B3LYP) level have been performed. Our results indicate that for large metal ions such as Pb(II) and Sr(II) the most stable conformation is $\Delta(\delta\lambda\delta)(\delta\lambda\delta)$, while for Ca(II) our calculations predict the $\Delta(\lambda\delta\lambda)(\lambda\delta\lambda)$ form being the most stable one. The selectivity that bp18c6^{2-} shows for Sr(II) over Ca(II) can be attributed to a better fit between the large Sr(II) ions and the relatively large crown fragment of the ligand. The X-ray crystal structure of the Pb(II) complex shows that the $\Delta(\delta\lambda\delta)(\delta\lambda\delta)$ conformation observed in solution is also maintained in the solid state. The Pb(II) ion is endocyclically coordinated, being directly bound to the 10 donor atoms of the ligand. The bond distances to the donor atoms of the pendant arms (2.55−2.60 Å) are substantially shorter than those between the metal ion and the donor atoms of the crown moiety (2.92−3.04 Å). This is a typical situation observed for the so-called hemidirected compounds, in which the Pb(II) lone pair is stereochemically active. The X-ray structures of the Zn(II) and Cd(II) complexes show that these metal ions are exocyclically coordinated by the ligand, which explains the high Pb(II)/Cd(II) and Pb(II)/Zn(II) selectivities. Our receptor bp18c6^{2-} shows promise for application in chelation treatment of metal intoxication by Pb(II) and ^{90}Sr(II).

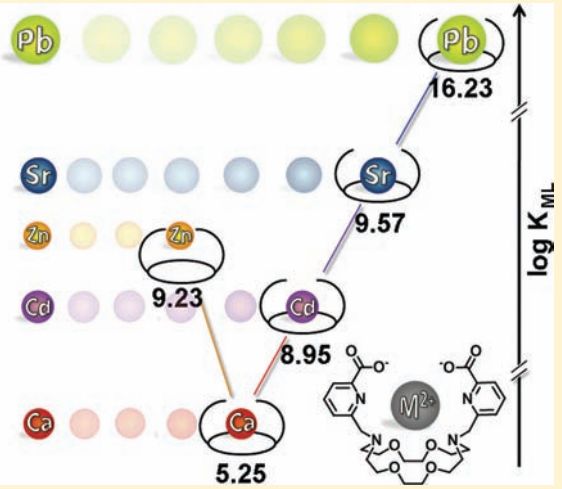

INTRODUCTION

An important field of application of chelate-forming compounds is the removal of toxic metal ions or radioactive isotopes from living organisms.[1] Indeed, extensive clinical experience demonstrated that the prognosis in acute and chronic intoxications with a range of metal ions can be improved considerably by administration of a suitable chelating agent.[2] A unique combination of features must be realized to design a ligand for application in chelation treatment of metal intoxication: (i) high thermodynamic stability of the complex formed with the target metal ion; (ii) fast rate of complexation with the metal ion of interest; (iii) high selectivity for the metal ion to be removed with respect to those essential in the vital processes (e.g., Zn(II), Cu(II), and Ca(II)); (iv) it should be nontoxic and should not be metabolized or excreted too rapidly; (v) suitable biodistribution to reach the deposits of the toxic metal in the body; (vi) the complex should be excretable and should be cleared promptly.[3] Ethylenediaminetetraacetic acid (edta), 2,3-mercaptopropanol (bal), dimercaptosuccinic acid (dmsa), and diethylenetriaminepentaacetic acid (dtpa) are the chelating agents widely used for removal of metal toxicity. However, most of these chelating agents suffer from some side effects, such as poor selectivity and high toxicity.[4]

Lead poisoning particularly affects young children who can absorb up to 50% of ingested lead.[5] Once ingested through the

Received: January 26, 2011
Published: March 17, 2011

Chart 1. Ligands Discussed in This Paper

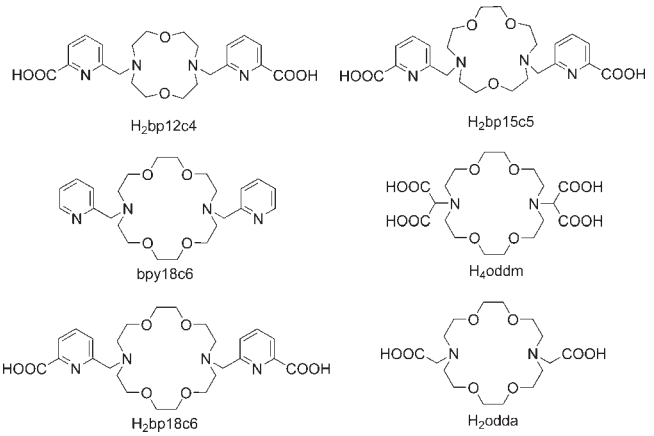

gastrointestinal track, lead accumulates in soft tissues including vital organs as kidneys, liver, or brain, where is bound to thiol and phosphate groups in proteins, nucleic acids, and cell membranes[6,7] originating severe neurological and/or hematological effects.[8] Among the drugs clinically administered at present for treatment of lead intoxication are $CaNa_2$edta,[9] dtpa,[10] and dmsa.[11]

Radioactive ^{90}Sr in the environment is also a matter of serious concern because of its relatively long half-life (28.8 years) and high energy of β-decay.[12] For instance, a large amount of radioactive ^{90}Sr was released following the nuclear reactor accident in Chernobyl.[13] After incorporation in the body, ^{90}Sr is accumulated in the bones originating severe adverse effects in human health.[14] Different approaches have been attempted to remove radioactive Sr fixed in the bones, including the use of chelating agents such as crown ethers, cryptands, and chelating agents such as edta and dtpa.[15] However, these studies have concluded that the radioactive Sr fixed in the bones is difficult to dislodge.[16] Part of these difficulties are attributed to the fact that many chelates, such as edta and dtpa, form more stable complexes with Ca(II) than with Sr(II). For a few cases in which a good Sr(II) to Ca(II) selectivity is observed,[17] the practical application is limited by the low rate of complexation of Sr(II). Thus, the discovery of chelating agents for the mobilization of strontium isotopes remains a challenging task for coordination chemists.

The cyclic framework of crown ethers provides an interesting platform for the complexation of different metal ions. Moreover, the relative facility with which crown ethers can be functionalized with pendant arm(s) containing additional donor atom(s) allows to enhance the cation binding ability and the selectivity of the parent crown ether.[18,19] The 18-membered ring of 4,13-diaza-18-crown-6 is known to be a useful platform for the design of selective ligands for large metal ions such as Pb(II) and Sr(II). Indeed, its 4,13-bis(acetic acid) derivative odda (Chart 1) shows a certain degree of selectivity for the large Pb(II) ion over Ca(II) and Zn(II), while the stabilities of the complexes formed with Sr(II) and Ca(II) are very similar.[20] An important improvement of the Sr(II)/Ca(II) selectivity is observed for the corresponding 7,16-bis(malonic acid) derivative oddm (Chart 1).[21] This ligand has been used in the preparation of sol−gel sorbents for Sr(II) separation.[22]

Keeping in mind these results, herein we have explored the potential use of the crown derivative *N,N′*-bis[(6-carboxy-2-pyridil)methyl]-4,13-diaza-18-crown-6 (H_2bp18c6, Chart 1) in chelation treatment of intoxication with large metal ions such as Pb(II) and Sr(II). In previous works we have reported the complexation properties of the related pendant crown ligands H_2bp12c4[23] and H_2bp15c5[24] toward divalent metal ions such as Pb(II), Cd(II), Zn(II), and Ca(II). We have shown that H_2bp12c4 forms stable complexes with these ions, the stability constants following the order Cd(II) > Zn(II) ∼ Pb(II) > Ca(II). As a consequence, H_2bp12c4 present an important Cd(II)/Ca(II) selectivity (6.14 log *K* units), as well as a certain selectivity for Cd(II) over Zn(II) (1.4 log *K* units). Increasing the macrocyclic ring size from H_2bp12c4 to H_2bp15c5 results in improved selectivities, the stability constants of H_2bp15c5 varying in the following order: Pb(II) > Cd(II) ≫ Zn(II) > Ca(II). In a recent paper, we have found that H_2bp18c6 shows an unprecedented selectivity for the large lanthanide(III) ions, with a dramatic drop of the stability being observed from Ce(III) to Lu(III) as the ionic radius of the lanthanide(III) ions decreases ($\log K_{CeL} - \log K_{LuL} = 6.9$).[25] This is in contrast to the stability trend observed for the H_2bp12c4 analogue, which does not show remarkable selectivity for a particular group of lanthanide ions.[26]

Thus, in the present paper we report a detailed investigation of the complexation properties of $bp18c6^{2-}$ toward Pb(II) and Sr(II) as well as toward some endogenously available metal ions such as Ca(II) and Zn(II). Thermodynamic stability constants of the different complexes of $bp18c6^{2-}$ have been determined by pH potentiometry. Aiming to rationalize their relative stability, the complexes were also studied by using ^1H and ^{13}C NMR techniques in D_2O solution. In addition, the Pb(II) and Sr(II) complexes were characterized by density functional theory (DFT) calculations carried out at the B3LYP level. The single crystal X-ray structures of the Zn(II), Cd(II), and Pb(II) complexes are also presented.

RESULTS

Ligand Protonation Constants and Stability Constants of the Metal Complexes. The protonation constants of $bp18c6^{2-}$ as well as the stability constants of its metal complexes formed with Sr(II), Ca(II), Zn(II), Cd(II), and Pb(II) were determined by potentiometric titration in 0.1 M KNO_3; the constants and standard deviations are given in Table 1, which also lists the protonation and stability constants reported for the related systems $edta^{4-}$, bpy18c6, $odda^{2-}$, and $oddm^{4-}$ (Chart 1). The ligand protonation constants are defined as in eq 1, and the stability constants of the metal chelates and the protonation constants of the complexes are expressed in eqs 2 and 3, respectively:

$$K_i = \frac{[H_iL]}{[H_{i-1}L][H^+]} \quad (1)$$

$$K_{ML} = \frac{[ML]}{[M][L]} \quad (2)$$

$$K_{MH_iL} = \frac{[MH_iL]}{[MH_{i-1}L][H^+]} \quad (3)$$

The ligand protonation constants determined in 0.1 M KNO_3 are very similar to those determined previously in 0.1 M KCl.[25] In

dx.doi.org/10.1021/ic200182e |*Inorg. Chem.* 2011, 50, 3772–3784

Table 1. Ligand Protonation Constants and Thermodynamic Stability Constants of $bp18c6^{2-}$ and Its Metal Complexes As Determined by pH-Potentiometry [I = 0.1 M KNO_3][a]

	$bp18c6^{2-}$	$bp15c5^{2-}$ [b]	$bp12c4^{2-}$ [c]	$odda^{2-}$ [d]	$oddm^{4-}$ [e]	$edta^{4-}$ [f]	bpy18c6[g]
log K_1	7.52(1)	8.21	8.67	8.45	7.95	10.19	7.44
log K_2	7.03(1)	7.19	6.90	7.80	7.35	6.13	6.26
log K_3	3.58(2)	3.43	3.42	2.90	3.03	2.69	1.38
log K_4	2.47(2)	2.53	1.67			2.00	
log K_{ZnL}	9.23(2)	11.14	15.48	8.42	6.25	16.5	6.96
log K_{ZnHL}	6.77(7)	4.33	2.31				
log K_{ZnH2L}	2.89(7)						
log K_{CdL}	8.95(1)	15.84	16.84	11.07	10.3	16.5	10.96
log K_{CdHL}	6.03(1)	2.62					
log K_{PbL}	16.23(7)	17.17	15.44	13.55	13.0	18.0	11.67
log K_{PbHL}	2.86(6)	2.52	2.52				
log K_{CaL}	5.25(6)	9.12	10.70	8.39	7.55	10.6	3.63
log K_{CaLH}		5.04	3.76				
log K_{CaH2L}		4.60					
log K_{SrL}	9.57(4)			8.29	9.79	8.68	
log K_{SrHL}	4.16(2)						

[a] Data reported previously for related systems are provided for comparison. [b] Ref 24. [c] Ref 23. [d] Ref 20. [e] Ref 21. [f] Ref 27. [g] Ref 30.

comparison to $edta^{4-}$,[27] $bp18c6^{2-}$ has a lower protonation constant for the first protonation step, while the second protonation constant is about 0.9 log K units lower in $edta^{4-}$ than in $bp18c6^{2-}$; these protonation processes occur on the amine nitrogen atoms. The higher protonation constant for the second protonation step of $bp18c6^{2-}$ in comparison to that of $edta^{4-}$ is attributed to a lower electrostatic repulsion between the two protonated amine nitrogen atoms in bp18c6 as consequence of the relatively long distance between them. In comparison to $odda^{2-}$,[20] $bp18c6^{2-}$ has lower protonation constants for the first and second protonation steps. This is in line with previous investigations, which showed that the replacement of the carboxylate groups of $edta^{4-}$ by pyridinecarboxylate units leads to a decrease in the basicity of the two amine nitrogen atoms.[28] The last two protonation steps are attributed to the protonation of the pyridylcarboxylate groups.[29] A comparison of protonation constants determined for $bp18c6^{2-}$ and those reported for bpy18c6[30] shows that the pyridylcarboxylate groups of $bp18c6^{2-}$ are considerably more basic than the pyridine units of bpy18c6.

Potentiometric titrations of $H_2bp18c6$ have been carried out in the presence of equimolar Sr(II), Ca(II), Zn(II), Cd(II), and Pb(II) ions to determine the stability constants of the corresponding metal complexes. Protonated forms of the complexes have been detected over the pH range studied for Sr(II), Zn(II), Cd(II), and Pb(II), while for the Ca(bp18c6) system, no evidence for the presence of protonated species has been obtained from the analysis of the potentiometric titration curves. Particularly high protonation constants have been obtained for the Zn(II) and Cd(II) complexes, the log K_{MLH} values amounting to 6.77 (Zn) and 6.03 (Cd). The solid state structures of these complexes show an exocyclic coordination of the metal ions in which amine nitrogen atoms are not involved in metal coordination (see below). Thus, the protonation of these complexes probably occurs in one of the uncoordinated amine nitrogen atoms. The species distribution diagrams calculated for the Zn(II), Cd(II), Sr(II), and Pb(II) complexes of $bp18c6^{2-}$ are depicted in Figure 1. The diagram obtained for Zn(II) shows the presence of about 6% of monoprotonated species at pH 8, while the diprotonated form of the complex is observed at pH < 5. In the case of the Cd(II) complex the protonated form of the complex is observed at pH < 8; The maximum concentration of the protonated form of the complex (ca. 88%) is reached at a pH of about 4.7. For the Sr(II) and Pb(II) complexes, the protonated forms of the complexes are observed at considerably lower pH (below ~6 and ~5 for Sr and Pb, respectively). These results indicate that the macrocyclic cavity of bp18c6 provides a good fit with the large Sr(II) and Pb(II) ions.

The $bp18c6^{2-}$ complex of Pb(II) shows the highest log K_{ML} value among the different divalent metal ions studied in this work. The log K_{PbL} value obtained for bp18c6 is considerably higher than those reported for bpy18c6, $odda^{2-}$, and $oddm^{4-}$, and about 1.8 log K units lower than that reported for $edta^{4-}$. The log K_{ML} values reported in Table 1 evidence an unprecedented selectivity of $bp18c6^{2-}$ for Pb(II) over Ca(II), Cd(II), and Zn(II), with $\Delta\log K_{ML} = \log K_{PbL} - \log K_{XL}$ values of 11.0 (X = Ca), 7.3 (X = Cd), and 7.0 (X = Zn). The speciation diagrams shown in Figure 1 highlight the selectivity of this ligand for Pb over Cd, Zn, and Ca. For instance, Pb(II) is almost totally complexed at pH 3 (99.1%), while only 70.5% of the total Zn(II), 24.6% of the total Cd(II), and 8×10^{-4}% of the total Ca(II) are complexed under the same conditions. Concerning the Sr(II)/Ca(II) selectivity, at pH 6.5 Sr(II) is almost totally complexed (99.6%), while only 60.1% of the total Ca(II) is complexed under the same conditions.

The thermodynamic stability constants alone are not sufficient to compare different complex stabilities under physiological conditions. The conditional stability constants, or more frequently the pM values, are considered to give a more realistic picture of complex stability. The pM values are usually defined as:

$$\mathrm{pM} = -\log[\mathrm{M}]_{\mathrm{free}} \quad \text{at} \quad \mathrm{pH} = 7.4 \quad \text{for} \quad [\mathrm{M(II)}] = 1\,\mu\mathrm{M}, \quad [\mathrm{L}] = 10\,\mu\mathrm{M}$$

The pM values obtained under these conditions for $bp18c6^{2-}$ complexes are compared to those of $edta^{4-}$, bpy18c6, $odda^{2-}$,

dx.doi.org/10.1021/ic200182e |Inorg. Chem. 2011, 50, 3772–3784

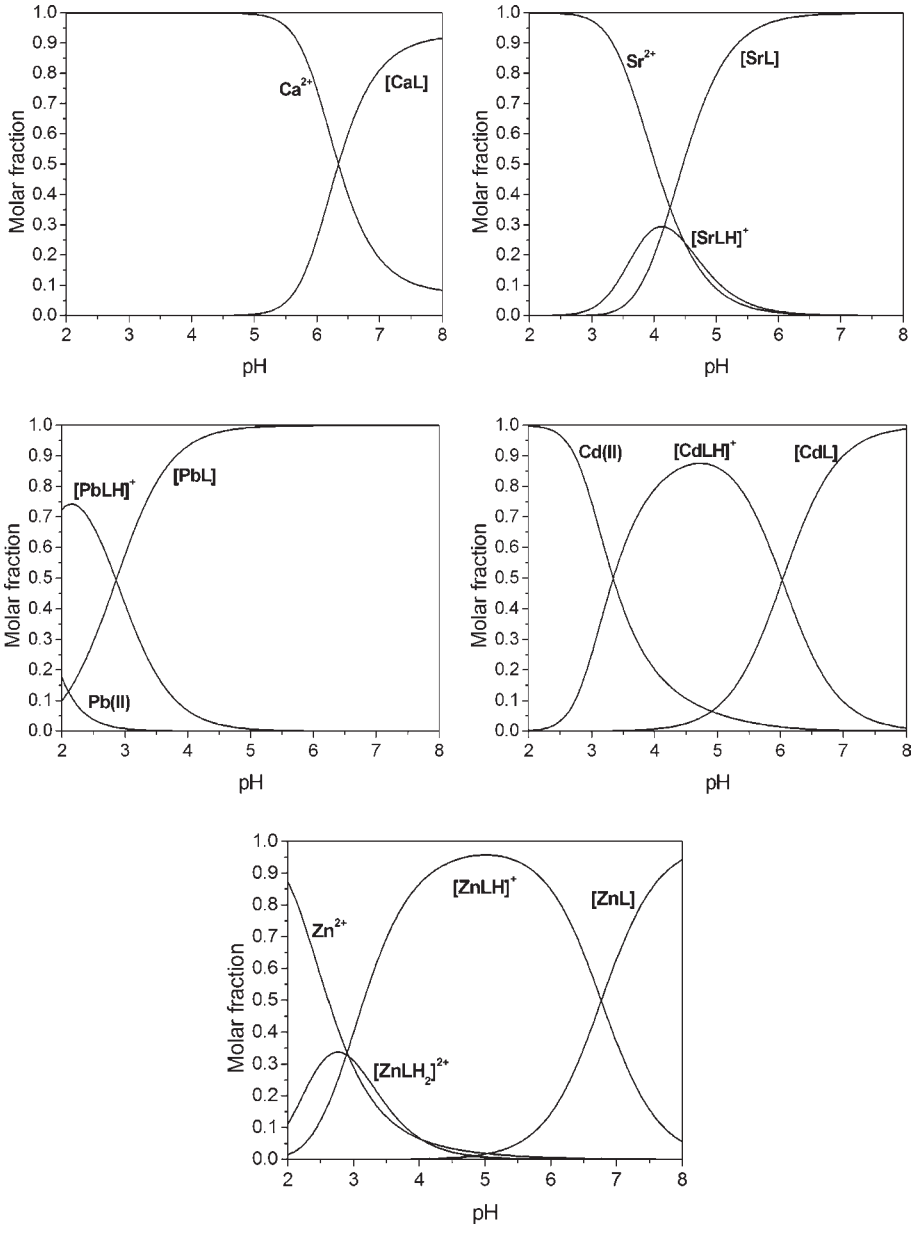

Figure 1. Species distribution diagrams of the Mbp18c6 systems (M = Zn, Cd, Sr, Ca, and Pb), 1:1 M(II):bp18c6^{2-}; [M(II)] = 1 mM; μ = 0.1 M KNO_3, 25 °C.

Table 2. pM Values[b] Obtained Determined by pH-Potentiometry [*I* = 0.1 M KNO_3] for [M(bp18c6)] Complexes (M = Zn, Cd, Pb, Sr, or Ca)[a]

	bp18c6^{2-}	bp15c5^{2-}	bp12c4^{2-}	odda^{2-}	oddm^{4-}	edta^{4-}	bpy18c6
Zn	9.8	11.0	15.0	7.8	6.5	14.6	7.1
Cd	9.5	15.7	16.4	10.4	10.4	14.6	11.0
Pb	16.7	17.1	15.0	12.9	13.1	16.1	11.7
Sr	10.1	*c*	*c*	7.6	9.9	6.9	*c*
Ca	6.2	9.0	10.2	7.7	7.6	8.7	6.0

[a] Data reported previously for related systems are provided for comparison. [b] pM values are defined as pM = -log$[M]_{free}$ at pH = 7.4 for [M(II)] = 1 μM, [L] = 10 μM. [c] Data not available.

and oddm^{4-} complexes in Table 2. The calculated pM values show that bp18c6^{2-} presents extremely high Sr(II)/Ca(II) and Pb(II)/Ca(II) selectivities. In fact, our ligand presents the best Pb(II)/Zn(II) and Pb(II)/Ca selectivities among the different ligands shown in Chart 1 (including edta^{4-}, which has been extensively used for the treatment of lead poisoning).[2] Moreover, bp18c6^{2-} shows the highest Sr(II)/Ca(II) selectivity reported so far.

X-ray Crystal Structures. The solid state structures of the Zn(II), Cd(II), and Pb(II) complexes of bp18c6^{2-} have been determined by X-ray diffraction studies. The Zn(II) complex **1** crystallizes in the monoclinic space group $P2_1$ and the asymmetric unit contains two different [Zn(bp18c6)(H_2O)] complex units with slightly different bond distances and angles. The crystal lattice also contains hydration water molecules that are involved in hydrogen-bonding interaction with oxygen atoms of the picolinate groups. Figure 2 shows a view of the structure of the complex, while selected bond lengths and angles of the metal

dx.doi.org/10.1021/ic200182e |*Inorg. Chem.* 2011, 50, 3772–3784

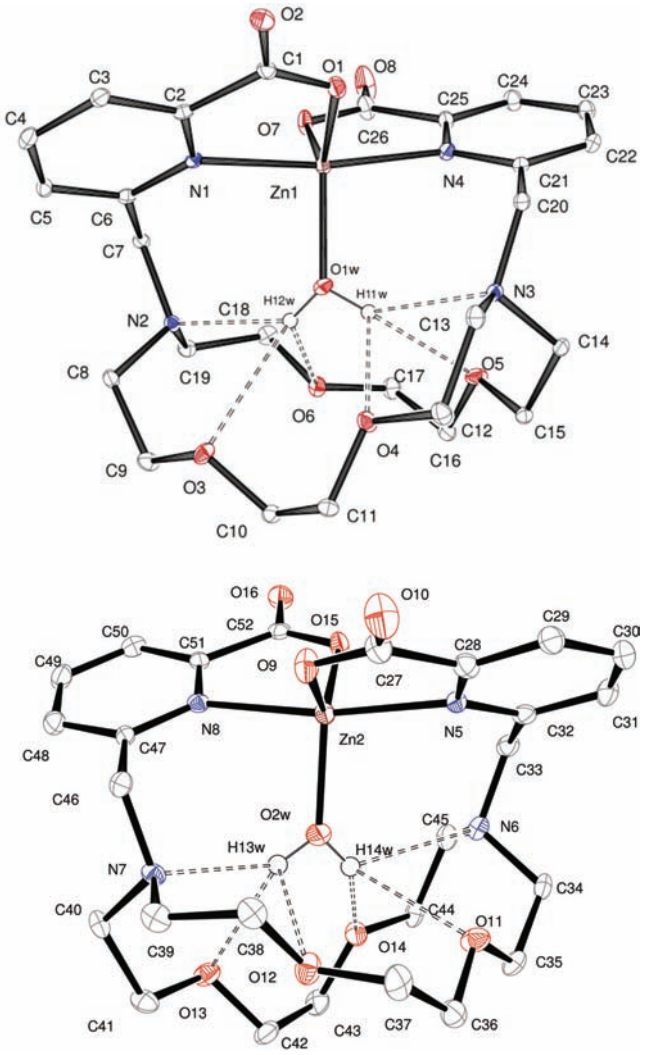

Figure 2. X-ray crystal structure of complex [Zn(bp18c6)(H_2O)] with atom labeling; hydrogen atoms are omitted for simplicity. The ORTEP plots are drawn at the 30% probability level.

coordination environment are given in Table 3. The ligand adopts a *syn* arrangement with both picolinate pendants being placed on the same side of the crown moiety. The Zn(II) ion is exocyclicly coordinated by the $bp18c6^{2-}$ ligand, being directly bound to the oxygen atoms of the carboxylate groups and to the pyridine nitrogen atoms. The donor atoms of the crown moiety remain uncoordinated. Exocyclic coordination of Zn(II) has been previously observed for complexes with a ligand derived from 4,13-diaza-18-crown-6 containing aniline pendant arms.[31] In [Zn(bp18c6)(H_2O)] the metal ion is five-coordinated, an oxygen atom of a water molecule occupying the fifth coordination position. The hydrogen atoms of the inner-sphere water molecule are involved in hydrogen bonding interaction with the six heteroatoms of the crown fragment (Figure 2). Hydrogen bonding data are summarized in the Supporting Information, Table S1. Inspection of the crystal structure reveals that weak face-to-face π,π-interactions are established between pyridyl units of adjacent [Zn(bp18c6)(H_2O)] entities.[32] The ligand molecules are stacked by pairs with the pyridine rings containing N1 and N8 lying nearly parallel to each other (2.69°). The distance between the centroids of these nearly parallel rings amounts to 3.90 Å.

Table 3. Selected Bond Lengths [Å] and Angles [deg] for [Zn(bp18c6)(H_2O)] in Compound 1[a]

Zn(1)−O(1W)	1.955(2)	Zn(2)−O(2W)	1.952(2)
Zn(1)−O(7)	1.987(2)	Zn(2)−O(15)	1.997(2)
Zn(1)−O(1)	2.002(2)	Zn(2)−O(9)	1.993(2)
Zn(1)−N(4)	2.132(2)	Zn(2)−N(8)	2.170(2)
Zn(1)−N(1)	2.152(2)	Zn(2)−N(5)	2.148(2)
O(1W)−Zn(1)−O(7)	117.39(9)	O(2W)−Zn(2)−O(9)	116.43(8)
O(1W)−Zn(1)−O(1)	120.64(9)	O(2W)−Zn(2)−O(15)	120.50(8)
O(7)−Zn(1)−O(1)	121.90(8)	O(9)−Zn(2)−O(15)	123.98(8)
O(1W)−Zn(1)−N(4)	97.79(8)	O(2W)−Zn(2)−N(5)	98.93(8)
O(7)−Zn(1)−N(4)	81.14(8)	O(9)−Zn(2)−N(5)	80.86(8)
O(1)−Zn(1)−N(4)	93.51(8)	O(15)−Zn(2)−N(5)	93.46(7)
O(1W)−Zn(1)−N(1)	90.38(8)	O(2W)−Zn(2)−N(8)	90.21(8)
O(7)−Zn(1)−N(1)	97.18(8)	O(9)−Zn(2)−N(8)	97.49(8)
O(1)−Zn(1)−N(1)	80.26(8)	O(15)−Zn(2)−N(8)	79.68(7)
N(4)−Zn(1)−N(1)	171.51(8)	N(5)−Zn(2)−N(8)	170.54(7)

[a] See Figure 2 for labeling.

The five coordinate Zn(II) ions are found in a slightly distorted trigonal bipyramidal coordination environment, as indicated from the value of the index of trigonality τ[33] of 0.90 and 0.92 for Zn(1) and Zn(2), respectively ($\tau = 0$ for a perfectly square pyramidal geometry and $\tau = 1$ for a regular trigonal bipyramidal geometry).[34] The two oxygen atoms of the carboxylate groups and the oxygen atom of the inner-sphere water molecule form the equatorial plane of the trigonal bipyramid, while the nitrogen atoms of the pyridine groups occupy the apical positions (Figure 2). The Zn(1) and Zn(2) atoms are placed only slightly above the plane defined by the three equatorial donor atoms (0.029 and 0.036 Å, respectively). The *trans* angles N(1)−Zn(1)−N(4) and N(8)−Zn(2)−N(5) [171.51(8) and 170.54(7)°, respectively] are relatively close to the expected value for a regular trigonal bipyramidal coordination (180°). The angles of the equatorial plane are also close to the ideal value of 120°, the larger deviation being observed for angle O(2W)−Zn(2)−O(9) [115.43(8)°]. The vectors defined by the metal ion and the axial donors form angles close to 90° with the vectors containing the metal ion and the equatorial donor atoms, as expected for a trigonal bipyramidal coordination environment. The largest deviation from the expected value is observed for the O(15)−Zn(2)−N(8) angle [79.68(7)°].

Crystals of the Cd(II) compound **2** contain the one-dimensional (1D) coordination polymer $[Cd(Hbp18c6)Cl]_n$. A view of the structure of the complex is shown in Figure 3, while bond distances of the metal coordination environment are given in Table 4. The analysis of the crystal structure shows that one of the pivotal nitrogen atoms [N(4), Figure 3] is protonated. The Cd(II) ion is exocyclically coordinated by the ligand, being simultaneously bound to the donor atoms of a picolinate unit of a $Hbp18c6^{+}$ ligand [N(1) and O(1)] and to those of a picolinate unit of a neighboring $Hbp18c6^{+}$ unit [N(3) and O(5)]. The metal ion is also directly bound to a nitrogen atom [N(2)] and an oxygen atom [O(3)] of one of the Hbp18c6 units. However, the Cd−O(3) distance [2.727(3) Å] is considerably longer than the distances to the remaining donor atoms of the ligand [2.25−2.52 Å]. Seven-coordination around the metal ion

dx.doi.org/10.1021/ic200182e |*Inorg. Chem.* 2011, 50, 3772–3784

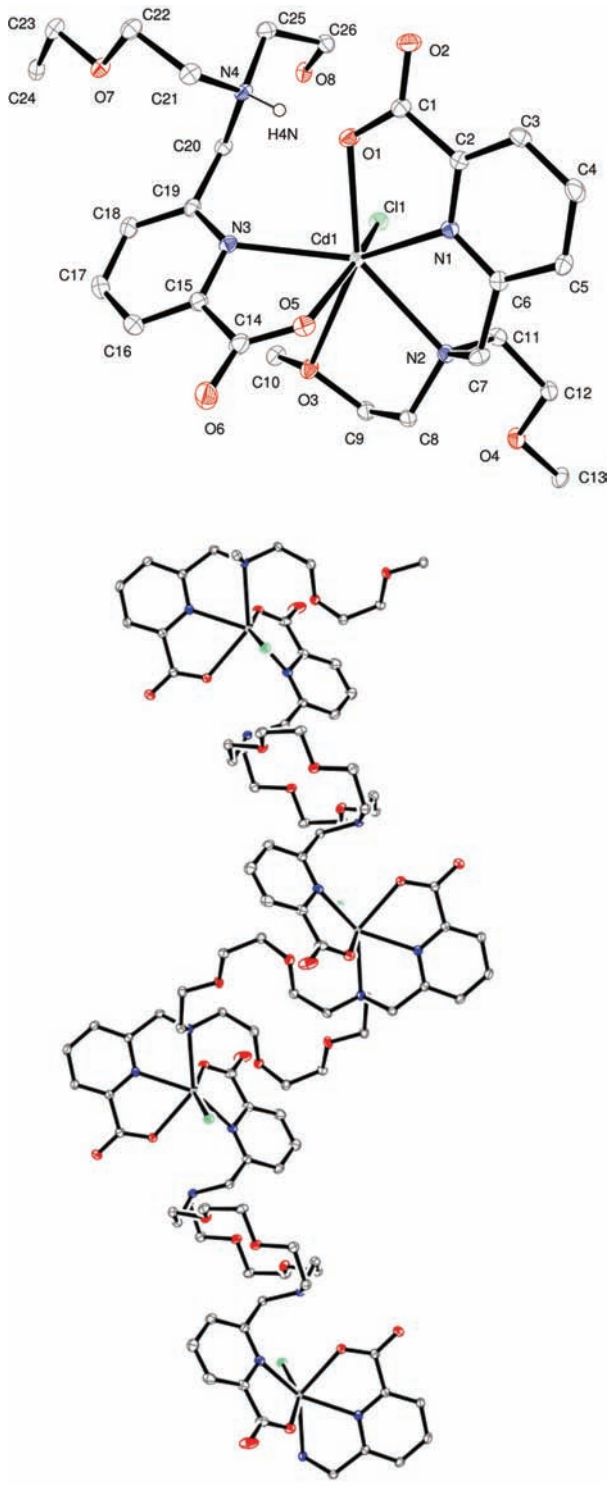

Figure 3. X-ray crystal structure of complex $[Cd(Hbp18c6)Cl]_n$ with atom labeling; hydrogen atoms are omitted for simplicity. The ORTEP plots are drawn at the 30% probability level. Top: asymmetric unit. Bottom: view of the 1D polymeric structure.

is completed by a chloride ligand. An oxygen atom of one of the picolinate units [O(1)] is involved in hydrogen bonding interaction with the protonated pivotal nitrogen atom: [N(4)···O(1) 2.639(4) Å, H(4N)···O(1) 1.73(4) Å, N(4)−H(4N)···O(1) 175(4)°]. As a consequence the Cd−O(1) bond distance [2.429(3) Å] is substantially longer than the Cd−O(5) one [2.258(3) Å].

Table 4. Selected Bond Lengths [Å] for [Cd(Hbp18c6)Cl] and [Pb(bp18c6)] Complexes in Compounds 2 and 3[a]

Cd(1)−O(5)	2.258(3)	Pb(1)−O(1)	2.550(2)
Cd(1)−N(1)	2.342(3)	Pb(1)−O(7)	2.558(2)
Cd(1)−O(1)	2.429(3)	Pb(1)−N(1)	2.585(3)
Cd(1)−Cl(1)	2.4695(9)	Pb(1)−N(4)	2.601(3)
Cd(1)−N(2)	2.503(3)	Pb(1)−O(3)	3.002(2)
Cd(1)−N(3)	2.516(3)	Pb(1)−O(4)	2.935(3)
Cd(1)−O(3)	2.727(3)	Pb(1)−N(3)	2.952(3)
		Pb(1)−N(2)	2.962(3)
		Pb(1)−O(6)	2.921(2)
		Pb(1)−O(5)	3.041(2)

[a] See Figures 3 and 4 for labeling.

Single crystals of formula $[Pb(bp18c6)]\cdot 2Et_3NHClO_4\cdot H_2O$ were obtained by slow evaporation of the mother liquor resulting from the reaction in 2-propanol of $H_2bp18c6\cdot 2HCl\cdot H_2O$ with the corresponding metal perchlorate in the presence of triethylamine. A view of the structure of the complex is shown in Figure 4, while bond distances and angles of the metal coordination environment are given in Table 4. The [Pb(bp18c6)] complex shows a slightly distorted C_2 symmetry in the solid state, where the symmetry axis is perpendicular to the pseudo-plane described by the four oxygen atoms of the crown moiety and contains the metal ion. The metal ion is directly bound to the 10 donor atoms of the ligand, but the bond distances to the donor atoms of the pendant arms (2.55−2.60 Å) are substantially shorter than those between the metal ion and the donor atoms of the crown moiety (2.92−3.04 Å, Table 4). This is typical of the so-called hemidirected compounds, in which the lone pair of electrons can cause a nonspherical charge distribution around the Pb(II) cation.[35,36] This results in the lengthening of the Pb-donor distances on the side where the stereochemically active Pb(II) lone pair is situated, which is accompanied by a concomitant shortening of the Pb-donor bond distances on the side of the Pb(II) ion away from it.[37] Several solid state structures of Pb(II) complexes with ligands derived from 4,13-diaza-18-crown-6 have been reported.[38] In these complexes, the distances between the metal ions and the donor atoms of the crown moiety are generally shorter than those observed for [Pb(bp18c6)], in line with the presence of a stereochemically active lone pair in the latter complex. This conclusion is also supported by DFT calculations (see below).

In the [Pb(bp18c6)] complex, the side arms of the ligand are placed above the plane of the macrocyclic unit, resulting in a *syn* conformation. Likewise, the lone pair of both pivotal nitrogen atoms is directed inward the receptor cavity in an *endo-endo* arrangement. The *syn* conformation of the ligand in these complexes implies the occurrence of two helicities, one belonging to the crown moiety (absolute configuration δ or λ) and one associated with the layout of the pendant arms (absolute configuration Δ or Λ).[39,40] Inspection of the crystal structure data reveals that, in the solid state, two $\Delta(\delta\lambda\delta)(\delta\lambda\delta)$ and $\Lambda(\lambda\delta\lambda)$-$(\lambda\delta\lambda)$ enantiomers cocrystallize in equal amounts (racemate). The coordination polyhedron around the Pb(1) ion in [Pb(bp18c6)] can be described as a severely distorted bicapped inverted-square antiprism composed of two parallel pseudo planes: O(1), N(4), O(4), and O(6) define the upper pseudo plane (mean deviation from planarity 0.179 Å), while O(7),

dx.doi.org/10.1021/ic200182e |*Inorg. Chem.* 2011, 50, 3772–3784

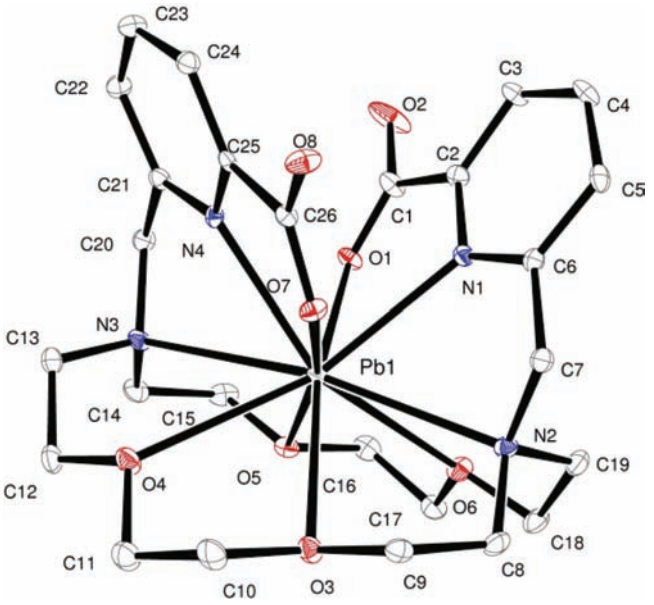

Figure 4. X-ray crystal structure of [Pb(bp18c6)] in **3** with atom labeling; hydrogen atoms are omitted for simplicity. The ORTEP plots are drawn at the 30% probability level.

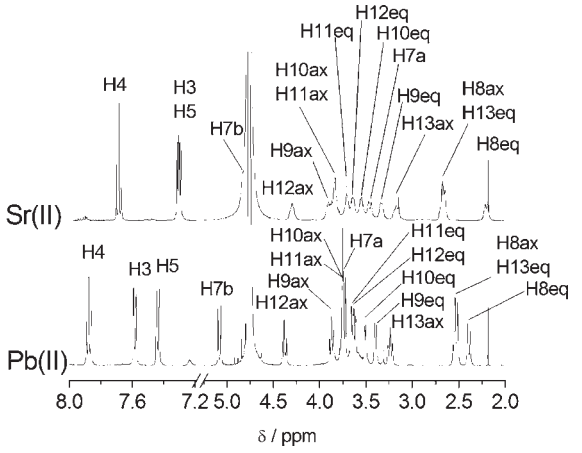

Figure 5. ^{1}H NMR spectra of the [M(bp18c6)] complexes (M = Sr or Pb) recorded in D_2O solution (pD = 7.0) at 298 K.

N(1), O(3), and O(5) define the lower pseudo plane (mean deviation from planarity 0.187 Å). The angle between these two least-squares planes amounts to 5.6°, and the Pb(1) ion is placed at 1.29 Å from the upper plane and 1.30 Å from the plane formed by O(7), N(1), O(3), and O(5). The mean twist angle, ω,[41] between these nearly parallel squares is 20.6°, a value that is close to that expected for an inverted square antiprism (ideal value 22.5°). The nitrogen atoms of the crown moiety [N(2) and N(3)] are capping, respectively, the lower and upper planes of the inverted-square antiprism, the N(2)−Pb(1)−N(3) angle amounting to 170.56(9)°.

^{1}H and ^{13}C NMR Spectra. The ^{1}H and ^{13}C NMR spectra of the [M(bp18c6)] complexes (M = Sr, Ca, Zn, Cd, or Pb) were obtained in D_2O solution at about pD = 7.0. Overall, the NMR spectra of the Pb(II) complex is consistent with the solid state structure of this complex described above. The proton spectra of the Sr(II) and Pb(II) complexes (Figure 5) consist of 17 signals

Chart 2. H_2bp18c6 Ligand and Its Numbering Scheme Used for NMR Spectral Assignment

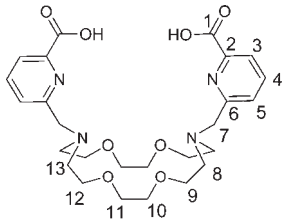

H_2bp18c6

Table 5. ^{1}H and ^{13}C NMR Shifts[a] of [M(bp18c6)] (M = Sr or Pb) Complexes[b]

^{1}H[c]	Sr	Pb[d]	^{13}C	Sr	Pb
H3	7.31	7.59	C1	172.8	173.6
H4	7.68	7.88	C2	152.5	151.4
H5	7.30	7.44	C3	126.6	128.6
H7a	3.47	3.75	C4	140.3	141.5
H7b	4.82	5.09	C5	122.8	124.7
H8ax	2.66	2.54	C6	159.6	160.6
H8eq	2.20	2.39	C7	62.0	61.0
H9ax	392	3.87	C8	55.5	56.3
H9eq	3.35	3.39	C9	70.1	70.0
H10ax	3.84	3.75	C10	71.5	71.6
H10eq	3.55	3.52	C11	71.4	71.1
H11ax	3.84	3.75	C12	70.1	68.7
H11eq	3.71	3.66	C13	55.1	55.1
H12ax	4.30	4.38			
H12eq	3.64	3.62			
H13ax	3.17	3.24			
H13eq	2.67	2.53			

[a] Parts per million (ppm) with respect to TMS. [b] See Chart 2 for labeling. [c] Assignment supported by 2D COSY, NOESY, HMQC, and HMBC experiments at 298 K. [d] $^{3}J_{3,4}$ = 7.7 Hz; $^{3}J_{5,4}$ = 7.6 Hz; $^{2}J_{7b,7a}$ = 15.6 Hz; $^{2}J_{8eq,8ax}$ = 14.0 Hz; $^{2}J_{9eq,9ax}$ = 10.5 Hz; $^{2}J_{10eq,10ax}$ = 8.5 Hz.

(see Chart 2 for labeling), pointing to an effective C_2 symmetry of the complexes in solution. This is also confirmed by the ^{13}C NMR spectra, which show 13 peaks for the 22 carbon nuclei of the ligand backbone. The ^{1}H spectrum of the Sr(II) complex shows relatively broad signals at room temperature, while the proton spectrum of the Pb(II) analogue displays sharp proton resonances. The assignments of the proton signals (Table 5) were based upon HMQC and HMBC two-dimensional (2D) heteronuclear experiments as well as standard 2D homonuclear COSY experiments, which gave strong cross-peaks between the geminal CH_2 protons (7−13) and between the ortho-coupled pyridyl protons. The signals due to protons H7a and H7b show an AB pattern where the larger shift for H7b results from the combined deshielding effects of the pyridyl ring current and the polarizing effect of the M(II) ion on the C−H bond pointing away from it.[42] The specific CH_2 proton assignments of the axial and equatorial H8−H13 protons were not possible on the basis of the 2D NMR spectra. However, it is known from previous ^{1}H NMR studies on complexes with macrocyclic ligands that the

dx.doi.org/10.1021/ic200182e |*Inorg. Chem.* 2011, 50, 3772–3784

ring axial protons experience strong coupling with the geminal protons and the vicinal axial protons, while the equatorial protons provide strong coupling with the geminal protons only.[43] Indeed, the $^3J_{H-H}$ coupling constants characterizing the coupling between vicinal pairs of protons (axial−axial, axial−equatorial, and equatorial−equatorial) follow the Karplus equation [$^3J_{H-H} = 7 - \cos\phi + 5\cos 2\phi$, where ϕ represents the H−C−C−H dihedral angle].[44] According to our DFT calculations (see below), the ϕ values involving axial−axial vicinal protons are close to 180° (167−176°), while the dihedral angles defined by axial−equatorial and equatorial−equatorial vicinal protons fall within the range 43−75°. Thus, the specific assignment of the axial and equatorial protons could be achieved in some cases by observing the coupling pattern of the proton signals. For instance, the signals due to protons H8 and H9 observed at 2.39 and 3.39 ppm in the spectrum of the Pb(II) complex (Figure 5) could be assigned to equatorial protons, as the spin coupling pattern is dominated by a $^2J_{H-H}$ of 10−14 Hz, the $^3J_{H-H}$ values being substantially smaller (<4 Hz). In other cases the assignments of the equatorial and axial protons could be achieved by observing the cross-peaks in the COSY spectra, as axial protons are expected to give two strong cross-peaks (geminal and axial−axial), whereas equatorial protons should show one strong (geminal) and two weak (equatorial−equatorial and equatorial−axial) cross-peaks.

The ^{1}H NMR spectra of the Zn(II), Cd(II), and Ca(II) complexes recorded at 298 K in D_2O solution show very broad featureless signals for the proton nuclei of the CH_2 groups. Decreasing the temperature to 278 K did not result in better resolved spectra. These results indicate a lower degree of complementary between the binding sites offered by the ligand and the small Zn(II), Cd(II), and even Ca(II) ions in comparison with the large Sr(II) and Pb(II) ones. A better resolved spectrum could be obtained in the case of the Zn(II) and Ca(II) complexes in CD_3OD solution at 198 K (see Supporting Information). However, the important broadening of the signals in the region 2−5 ppm indicates that the slow exchange region is not achieved even at low temperature. The broadening of many of the proton signals did not allow a full assignment of the proton spectra, which are consistent with a C_2 symmetry in solution. This is again confirmed by the ^{13}C NMR spectrum, which shows 13 peaks for the 22 carbon nuclei of the ligand backbone. The C_2 symmetry observed for the Zn(II) complex at low temperature, together with the flexibility of the crown moiety, is in agreement with the exocyclic coordination of the metal ion observed in the solid state (see above).

Conformational Analysis. ^{1}H and ^{13}C NMR spectra recorded for the Sr(II) and Pb(II) complexes of bp18c6 indicate a relatively rigid C_2 symmetry of the complexes in solution. Thus, to obtain information about the structure in solution of these complexes, the [M(bp18c6)] systems (M = Sr or Pb) were investigated by means of DFT calculations (B3LYP model). In these calculations, the 6-31G(d) basis set was used for the ligand atoms, while for the metals the effective core potential of Wadt and Hay (Los Alamos ECP) included in the LanL2DZ basis set was applied. Compared to all-electron basis sets ECPs account for relativistic effects to some extent. It is believed that relativistic effects will become important for the elements from the fourth row of the periodic table. A detailed analysis of the coordinative properties of the bp18c6 ligand showed that there are 16 possible conformations of the complexes of bp18c6 (eight enatiomeric pairs of diasteroisomers) consistent with a C_2 symmetry.[25] Since enantiomers have the same physicochemical properties in a nonchiral environment, we have only considered in our conformational analysis the 8 diasteroisomeric forms of the complexes given in Table 6. Optimized Cartesian coordinates for the different [M(bp18c6)] complexes are given in the Supporting Information (M = Sr or Pb). All the optimized geometries indeed show a nearly undistorted C_2 symmetry. Full geometry optimization of each conformation performed in vacuo was followed by single point energy calculations in aqueous solution. The in aqueous solution relative energies of the different conformations are given in Table 6.

Table 6. Relative Free Energies [kcal·mol^{-1}] in Aqueous Solution [C-PCM, B3LYP/6-31G(d)] of Different Conformations of [M(bp18c6)] (M = Sr or Pb) Complexes with C_2 Symmetry

	Sr	Pb		Sr	Pb
$\Delta(\lambda\lambda\lambda)(\lambda\lambda\lambda)$	6.26	6.74	$\Delta(\lambda\lambda\delta)(\lambda\lambda\delta)$	7.80	9.14
$\Delta(\delta\delta\delta)(\delta\delta\delta)$	5.30	6.66	$\Delta(\delta\delta\lambda)(\delta\delta\lambda)$	4.18	7.08
$\Delta(\delta\lambda\lambda)(\delta\lambda\lambda)$	3.71	6.67	$\Delta(\lambda\delta\delta)(\lambda\delta\delta)$	7.38	8.55
$\Delta(\lambda\delta\lambda)(\lambda\delta\lambda)$	1.40	2.96	$\Delta(\delta\lambda\delta)(\delta\lambda\delta)$	0.00	0.00

Our DFT calculations show that in both Pb(II) and Sr(II) complexes two of the conformations, $\Delta(\delta\lambda\delta)(\delta\lambda\delta)$ and $\Delta(\lambda\delta\lambda)(\lambda\delta\lambda)$, are significantly more stable than the remaining six conformations with C_2 symmetry. Previous studies on the lanthanide complexes of bp18c6^{2-} have demonstrated that for the largest La(III) ion the most stable conformation is the $\Delta(\delta\lambda\delta)(\delta\lambda\delta)$ one, while for Nd−Lu the minimum energy conformation corresponds to the $\Delta(\lambda\delta\lambda)(\lambda\delta\lambda)$ form.[25] The in aqueous solution minimum energy conformation predicted by our DFT calculations for the Pb(II) and Sr(II) complexes corresponds to that found in solution for the larger lanthanide ions, which is the same conformation observed for the [Pb(bp18c6)] complex in the solid state ($\Delta(\delta\lambda\delta)(\delta\lambda\delta)$, see above). The ionic radius of Sr(II) determined for CN 10 (1.36 Å) is only slightly larger than that of La(III) (1.27 Å),[45] while the ionic radius of Pb(II) for CN 10 is even larger (1.40 Å). Thus, it is not surprising that the Pb(II) and Sr(II) complexes adopt the same conformation observed for the large lanthanide(III) ions. Even so, our calculations predict an important stabilization (ca. 1.7 kcal·mol^{-1}) of the $\Delta(\lambda\delta\lambda)(\lambda\delta\lambda)$ form with respect to the $\Delta(\delta\lambda\delta)(\delta\lambda\delta)$ one upon decreasing the ionic radius of the metal ion from Pb(II) to Sr(II) (Table 6).

The in vacuo optimized bond distances of the metal coordination environments obtained for the minimum energy conformations of [M(bp18c6)] (M = Pb or Sr) complexes are given in Table 7. The distances between Sr(II) and the donor atoms of the pendant arms are considerably longer than those obtained for the Pb(II) analogue, while the distances to the donor atoms of the crown moiety are considerably longer for the Pb(II) complex than for the Sr(II) one. These results suggest that the Pb(II) lone pair in [Pb(bp18c6)] is stereochemically active, that is, the lone pair of electrons causes a nonspherical charge distribution around the Pb(II) cation. This results in the lengthening of the Pb-donor distances on the side where the stereochemically active Pb(II) lone pair is situated (the crown moiety), which is accompanied by a concomitant shortening of the Pb-donor bond distances on the side of the Pb(II) ion away from the site of the stereochemically active lone pair (the donor atoms of the pendant arms). An analysis of the natural bond orbitals

dx.doi.org/10.1021/ic200182e |Inorg. Chem. 2011, 50, 3772–3784

Table 7. Bond Distances (Å) of the Metal Coordination Environments for [M(bp18c6)] (M = Pb or Sr) Complexes Calculated at the B3LYP/6-31G(d) Level[a]

	M−N_{PY}	M−O_{COO}	M−O_C[b]	M−O_C[b]	M−N_{AM}
Pb	2.594	2.322	3.176	3.244	3.177
Sr	2.744	2.548	2.859	2.990	3.089

[a] Data obtained for the $\Delta(\delta\lambda\delta)(\delta\lambda\delta)$ conformations are given. N_{AM} = amine nitrogen atoms; N_{PY} = pyridyl nitrogen atoms; O_{COO} = carboxylate oxygen atoms; O_C = crown oxygen atoms. [b] The optimized geometries show two different M−O_C bond distances, as expected for a C_2 symmetry.

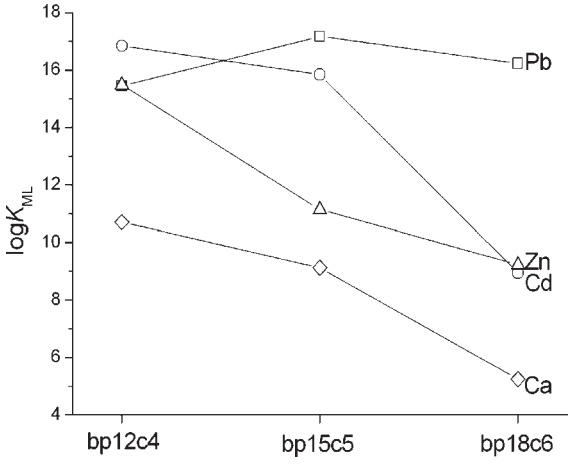

Figure 6. Comparison of the log K_{ML} values for the Zn(II), Cd(II), Pb(II), and Ca(II) complexes of $bp12c4^{2-}$, $bp15c5^{2-}$, and $bp18c6^{2-}$ [μ = 0.1 M KNO_3, 25 °C].

(NBOs) in [Pb(bp18c6)] shows that the Pb(II) lone pair orbital possesses a predominant 6s character, but it is polarized by a substantial 6p contribution: s[97.45%]p[2.55%]. Similar p contributions (1.89−4.39%) have been calculated for different hemidirected four-coordinate Pb(II) complexes with neutral ligands, while p contributions in the range 2.62−15.72% have been calculated for hemidirected four-coordinate Pb(II) complexes with anionic ligands.[35] Compared to the Pb-donor distances observed in the solid state, our calculations overestimate the distances to donor atoms of the crown moiety by 0.22−0.25 Å, while the calculated distances between the Pb(II) ion and the oxygen atoms of picolinate groups are about 0.23 Å shorter than those observed in the solid state. These results indicate that the structure of [Pb(bp18c6)] optimized in the gas phase presents a more important degree of sterochemical activity of the Pb(II) lone pair than the structure observed in the solid state. Geometry optimizations performed in aqueous solution (PCM model) on the $\Delta(\delta\lambda\delta)(\delta\lambda\delta)$ form of [Pb(bp18c6)] show that the inclusion of solvent effects has a small impact on the calculated Pb-donor distances (<0.044 Å), which suggests that the stereochemical activity of the Pb(II) lone pair is also present in the solution state.

DISCUSSION AND CONCLUSIONS

Figure 6 shows a comparison of the log K_{ML} values for the Zn(II), Cd(II), Pb(II), and Ca(II) complexes of receptor $bp18c6^{2-}$ and the related $bp12c4^{2-}$ and $bp15c5^{2-}$ previously reported by us.[23,24] (Data given in Table 1). Increasing the size of the crown moiety from $bp12c4^{2-}$ to $bp15c5^{2-}$ causes a dramatic drop of the stability of the Zn(II) complex, while the stabilities of the Cd(II) and Ca(II) complexes decrease to a lower extent. A further increase of the macrocyclic ring size causes an additional drop of the complex stability for Zn(II), and a dramatic decrease of the stability of the complexes formed with Cd(II) and Ca(II). The stability of the complexes formed with Cd(II) and Ca(II) as a function of ring size follows similar trends, which is not unexpected considering the similarity in the eight-coordinate effective ionic radii of Cd(II) (1.10 Å) and Ca(II) (1.12 Å).[45] In contrast to the situation observed for Zn(II), Cd(II), and Ca(II), the stability of the Pb(II) complexes is relatively insensitive to macrocyclic size variation. This is attributed to the plasticity of the Pb(II) coordination environment related to the stereochemical activity of the 6s lone pair. Indeed, it is well-known that Pb(II) can vary in size to a certain extent depending on whether the 6s lone-pair is stereochemically active or not, a stereochemically active lone pair considerably decreasing the ionic radius of the metal ion.[46]

The dramatic drop of complex stability in [Zn(bp15c5)] compared with [Zn(bp12c4)], and in [Cd(bp18c6)] compared with [Cd(bp15c5)], may be attributed to the so-called *dislocation discrimination*.[47] Dislocation discrimination is associated with a sudden change in coordination behavior of a particular metal ion along a series of closely related macrocyclic ligands. In principle, a dislocation will occur when the gradation of ligand properties along the series results in a sudden destabilization of one complex structure relative to a second one. Our previous studies have shown that in the [Zn(bp12c4)] complex the metal ion is endocyclically coordinated by the ligand, which results in a relatively rare eight-coordinated Zn(II) complex.[23] The solid state structure of [Zn(bp18c6)(H_2O)] herein reported shows that the metal ion is exocyclically coordinated by the ligand. An exocyclic coordination of Zn(II) by bp15c5 was also proposed on the basis of DFT calculations.[24] These structural data clearly confirm that a sudden change in coordination behavior occurs upon increasing the macrocyclic ring size from $bp12c4^{2-}$ to $bp15c5^{2-}$, which it is reflected in a dramatic drop of the corresponding stability constants. The larger ionic radius of Cd(II) allows an endocyclic coordination of this metal ion by both $bp12c4^{2-}$ and $bp15c5^{2-}$, as evidenced by the corresponding solid state structures.[23,24] The macrocyclic cavity of $bp18c6^{2-}$ is, however, too large to provide a good fit with Cd(II), which results in an exocyclic coordination of this metal ion. This again provokes a sharp decrease of complex stability upon increasing the macrocyclic cavity size from $bp15c5^{2-}$ to $bp18c6^{2-}$. A similar structural change is probably responsible for the stability sequence observed for the complexes of Ca(II).

In conclusion, in this paper we have presented a rationalized study of the complexation properties of the macrocyclic decadentate receptor $bp18c6^{2-}$ toward several divalent metal ions. We have found that this ligand is especially suited for the complexation of large metal ions such as Sr(II) and Pb(II), which results in very high Pb(II)/Ca(II) and Pb(II)/Zn(II) selectivities (in fact, higher than those found for ligands widely used for the treatment of lead poisoning such as edta), as well as in the highest Sr(II)/Ca(II) selectivity reported so far. Thus, our receptor bp18c6 shows promise for application in chelation treatment of metal intoxication by Pb(II) and ^{90}Sr(II).

EXPERIMENTAL SECTION

Solvents and Starting Materials. *N,N′*-Bis[(6-carboxy-2-pyridil)methyl]-4,13-diaza-18-crown-6 (H_2bp18c6) was prepared as

dx.doi.org/10.1021/ic200182e |*Inorg. Chem.* 2011, 50, 3772–3784

previously reported by us.[25] All other chemicals were purchased from commercial sources and used without further purification, unless otherwise stated.

Caution! *Although we have experienced no difficulties with the perchlorate salts, these should be regarded as potentially explosive and handled with care.*[48]

[Zn(bp18c6)]. Triethylamine (0.167 g, 1.650 mmol) was added to a suspension of H_2bp18c6·4HCl·5H_2O (0.210 g, 0.270 mmol) in 2-propanol (5 mL). The mixture was heated to reflux with stirring for a period of 0.5 h, and then a solution of $Zn(ClO_4)_2·6H_2O$ (0.130 g, 0.349 mmol) in the same solvent (5 mL) was added. The resultant solution was heated to reflux for 1.5 h, filtered, and the filtrate concentrated to about 3 mL. Addition of diethylether resulted in the formation of a white solid, which was collected by filtration and dried under vacuum (yield 0.110 g, 68%). HR-MS (ESI^+) calcd. for $[C_{26}H_{35}N_4O_8Zn]^+$ 595.1741; found 595.1740. IR: 1630 ν(C═O), 1592 $\nu(C{=}N)_{py}$ cm^{-1}. Slow evaporation of the mother-liquor gave single crystals of formula [Zn(bp18c6)(H_2O)]·2.5H_2O (**1**) suitable for X-ray diffraction analyses.

[Cd(bp18c6)]. The preparation of this compound followed the same procedure as that described for the Zn(II) analogue by using triethylamine (0.261 g, 2.583 mmol), H_2bp18c6·4HCl·5H_2O (0.330 g, 0.425 mmol), and $Cd(ClO_4)_2$ (0.170 g, 0.546 mmol) in 10 mL of 2-propanol (yield 0.160 g, 59%). HR-MS (ESI^+) calcd. for $[C_{26}H_{35}CdN_4O_8]^+$ 645.1483; found 645.1483. IR: 1629 ν(C═O), 1586 $\nu(C{=}N)_{py}$ cm^{-1}. Slow evaporation of the mother-liquor gave single crystals of formula [Cd_2(Hbp18c6)($Cl)_2$]·4^{i}PrOH·5H_2O (**2**) suitable for X-ray diffraction analyses.

[Pb(bp18c6)]. Triethylamine (0.167 g, 1.650 mmol) was added to a suspension of H_2bp18c6·4HCl·5H_2O (0.210 g, 0.270 mmol) in 2-propanol (5 mL). The mixture was heated to reflux with stirring for a period of 0.5 h, and then a solution of $Pb(ClO_4)_2·3H_2O$ (0.130 g, 0.283 mmol) in the same solvent (5 mL) was added. The resultant solution was heated to reflux for 1.5 h, filtered, and the filtrate concentrated to about 3 mL. Addition of diethylether resulted in the formation of a white solid, which was collected by filtration and dried under vacuum (yield 0.120 g, 60%). HR-MS (ESI^+) calcd. for $[C_{26}H_{35}N_4O_8Pb]^+$ 739.2216; found 739.2215. IR: 1610 ν(C═O), 1580 $\nu(C{=}N)_{py}$ cm^{-1}. Slow evaporation of the mother-liquor gave single crystals of formula [Pb(bp18c6)]·2Et_3NHClO_4·H_2O (**3**) suitable for X-ray diffraction analyses.

[Ca(bp18c6)]. The preparation of this compound followed the same procedure as that described for the Pb(II) analogue by using triethylamine (0.245 g, 2.439 mmol), H_2bp18c6·4HCl·5H_2O (0.310 g, 0.399 mmol), and $Ca(ClO_4)_2·4H_2O$ (0.150 g, 0.482 mmol) in 10 mL of 2-propanol (yield 0.180 g, 79%). HR-MS (ESI^+) calcd. for $[C_{26}H_{35}CaN_4O_8]^+$ 571.2075; found 571.2075. IR: 1623 ν(C═O), 1589 $\nu(C{=}N)_{py}$ cm^{-1}.

[Sr(bp18c6)]. The preparation of this compound followed the same procedure as that described for the Pb(II) analogue by using triethylamine (0.247 g, 2.439 mmol), H_2bp18c6·4HCl·5H_2O (0.310 g, 0.399 mmol), and $Sr(ClO_4)_2·H_2O$ (0.130 g, 0.427 mmol) in 10 mL of 2-propanol (yield 0.230 g, 93%). HR-MS (ESI^+) calcd. for $[C_{26}H_{35}N_4O_8Sr]^+$ 619.1506; found 619.1505. IR: 1717 ν(C═O), 1591 $\nu(C{=}N)_{py}$ cm^{-1}.

General Methods. ^{1}H and ^{13}C NMR spectra were recorded at 25 °C on Bruker Avance 300 and Bruker Avance 500 MHz spectrometers. For measurements in D_2O, *tert*-butyl alcohol was used as an internal standard with the methyl signal calibrated at δ = 1.2 (^{1}H) and 31.2 ppm (^{13}C). Spectral assignments were based in part on 2D COSY, HMQC, and HMBC experiments. High resolution ESI-TOF mass spectra were recorded using a LC-Q-q-TOF Applied Biosystems QSTAR Elite spectrometer in the positive mode. IR spectra were recorded using a Bruker Vector 22 spectrophotometer equipped with a Golden Gate Attenuated Total Reflectance (ATR) accessory (Specac).

Potentiometric Titrations. Ligand protonation constants and stability constants with Zn(II), Cd(II), Pb(II), Sr(II), and Ca(II) were determined by pH-potentiometric titration at 25 °C in 0.1 M KNO_3. The samples (10 mL) were stirred while a constant Ar flow was bubbled through the solutions. The titrations were carried out adding a standardized KOH solution with a Metrohm Dosimat 794 automatic buret. KOH was standarized by potentiometric titration against potassium hydrogen phthalate. A glass electrode filled with 3 M KCl was used to measure pH. The stock solutions of MCl_2 (M = Sr, Ca, Zn or Cd) and $Pb(NO_3)_2$ were prepared by dilution of the appropriate standards (Aldrich). The pH of the titration mixture was adjusted by addition of a known volume of standard HNO_3. The exact amount of acid present in the standard solutions was determined by pH measurement. H_2bp18c6 was checked for purity by NMR and elemental analysis before titration. The ligand and metal−ligand (1:1) solutions were titrated over the pH range 2 0.0 < pH < 11.0. In the case of the metal−ligand (1:1) solutions reverse titrations were performed to check the reversibility of the system. Reverse titrations were carried out adding a standardized HNO_3 solution; the pH of the titration mixture was adjusted by addition of a known volume of standard KOH. The protonation and stability constants were calculated from simultaneous fits of three independent titrations with the program HYPERQUAD.[49] The errors given correspond to one standard deviation.

X-ray Crystal Structures. Three dimensional X-ray data were collected on a Bruker X8 APEXII CCD for **2** and **3** complexes and on a Bruker Smart 1000 CCD for **1**. All three data sets were corrected for Lorentz and polarization effects and for absorption by semiempirical methods[50] based on symmetry-equivalent reflections. Complex scattering factors were taken from the program SHELX97[51] running under the WinGX program system[52] as implemented on a Pentium computer. All the structures were solved by Patterson methods (DIRDIF-2008 for the **2** and **3** complexes and SHELXS97 for **1**),[51,53] and refined by full-matrix least-squares on F^2. All hydrogen atoms were included in calculated positions and refined in riding mode for all compounds, except those of the solvent water molecules present in all crystals that were located using CALC−OH,[54] and all the positional parameters fixed. The coordinated water molecules present in the **1** were found in a difference Fourier map and all the parameters fixed. Finally, the protons bound to the pivotal nitrogen atoms in one of the macrocyclic units of **2** were found in a difference Fourier map as well, but the position was refined freely. Refinement converged with anisotropic displacement parameters for all non-hydrogen atoms. Crystal data and details on data collection and refinement are summarized in Table 8.

Computational Methods. All calculations were performed employing hybrid DFT with the B3LYP exchange-correlation functional,[55,56] and the Gaussian 03 package (Revision C.01).[57] Full geometry optimizations of the [M(bp18c6)] systems (M = Sr or Pb) systems were performed in vacuo by using the standard 6-31G(d) basis set for the ligand atoms and the LanL2DZ valence and effective core potential functions for the metals.[58] The stationary points found on the potential energy surfaces as a result of the geometry optimizations have been tested to represent energy minima rather than saddle points via frequency analysis. In aqueous solution relative free energies of the different conformations of the complexes were calculated from solvated single point energy calculations on the geometries optimized in vacuo. In these calculations solvent effects were evaluated by using the polarizable continuum model (PCM). In particular, we used the C-PCM variant[59] that employs conductor rather than dielectric boundary conditions. The solute cavity is built as an envelope of spheres centered on atoms or atomic groups with appropriate radii. Calculations were performed using an average area of 0.2 Å^2 for all the finite elements (tesserae) used to build the solute cavities. Free energies include both electrostatic and non-electrostatic contributions and non-potential energy terms (that is, zero point energies and thermal terms) obtained from frequency analysis

Table 8. Crystal Data and Refinement Details for 1, 2, and 3

	1	2	3
formula	$C_{52}H_{82}N_8O_{23}Zn_2$	$C_{64}H_{112}Cd_2Cl_2N_8O_{25}$	$C_{76}H_{134}Cl_4N_{12}O_{33}Pb_2$
MW	1318.00	1689.32	2300.13
crystal system	monoclinic	triclinic	monoclinic
space group	$P2_1$	$P\bar{1}$	$P2_1/n$
T/K	100.0(2)	100.0(2)	100.0(2)
a/Å	9.8857(7)	11.8366(4)	9.1268(4)
b/Å	15.837(1)	12.0850(4)	48.474(2)
c/Å	19.114(1)	14.9182(5)	10.8772(4)
α/deg	90	100.066(2)	90
β/deg	97.081(2)	108.711(2)	96.307(2)
γ/deg	90	94.059(2)	90
V/Å^3	2969.7(3)	1971.58(11)	4783.1(3)
F(000)	1388	882	2340
Z	2	1	2
λ, Å (MoK$_\alpha$)	0.71073	0.71073	0.71073
D_{calc}/g cm^{-3}	1.474	1.423	1.597
μ/mm^{-1}	0.894	0.684	3.712
θ range/deg	2.79−28.33	2.69−28.38	2.27−28.31
R_{int}	0.0339	0.0643	0.0453
reflns measd	42468	35152	47240
unique reflns	14465	9782	11880
reflns obsd	13005	7241	9559
GOF on F^2	1.04	1.064	1.053
R_1[a]	0.0321	0.0506	0.0382
wR_2 (all data)[b]	0.0790	0.1350	0.0645
largest differences peak and hole/e Å^{-3}	0.791	1.047	1.045
	0.464	0.811	−1.561

[a] $R_1 = \Sigma||F_o| - |F_c||/\Sigma|F_o|$. [b] $wR_2 = \{\Sigma[w(|F_o|^2 - |F_c|^2)^2]/\Sigma[w(F_o^4)]\}^{1/2}$.

performed in vacuo. The wave functions of the [Pb(bp18c6)] complex were analyzed by natural bond orbital analyses, involving natural atomic orbital (NAO) populations and natural bond orbitals (NBO).[60,61]

■ ASSOCIATED CONTENT

Supporting Information. Experimental potentiometric curves, in vacuo optimized Cartesian coordinates for the [M(bp18c6)] systems (M = Pb or Sr), and X-ray crystallographic data in CIF format. This material is available free of charge via the Internet at http://pubs.acs.org.

■ AUTHOR INFORMATION

Corresponding Author

*E-mail: teresa.rodriguez.blas@udc.es (T.R.-B.), carlos.platas.iglesias@udc.es (C.P.-I.).

■ ACKNOWLEDGMENT

The authors thank Xunta de Galicia (PGIDIT06TAM10-301PR and IN845B-2010/063) for generous financial support. The authors are indebted to Centro de Supercomputación de Galicia (CESGA) for providing the computer facilities.

■ REFERENCES

(1) Blanusa, M.; Varnai, V. M.; Piasek, M.; Kostial, K. *Curr. Med. Chem.* **2005**, *12*, 2771–2794.

(2) Andersen, O. *Chem. Rev.* **1999**, *99*, 2683–2710.

(3) Andersen, O. *Mini Rev. Med. Chem.* **2004**, *4*, 11–21.

(4) Aposhian, H. V.; Maiorino, R. M.; Gonzalez-Ramirez, D.; Zuniga-Charles, M.; Xu, Z.; Hurlbut, K. M.; Junco-Munoz, P.; Dart, R. C.; Aposhian, M. M. *Toxicology* **1995**, *97*, 23–38.

(5) Goyer, R. A. In *Handbook on Toxicity of Inorganic Compounds*; Seiler, H. G., Sigel, A., Sigel, H., Eds.; Marcel Dekker: New York, 1988; pp 359−382.

(6) (a) Sigel, H.; Da Costa, C. P.; Martin, R. B. *Coord. Chem. Rev.* **2001**, *219−221*, 435–461. (b) Sigel, B. E.; Fischer, H.; Farkas, E. *Inorg. Chem.* **1983**, *22*, 925–934. (c) Tajimir-Riahi, H. A.; Langlais, M.; Savoie, R. *Nucleic Acids Res.* **1988**, *16*, 751–762.(d) Kazantis, G. In *Poisoning, Diagnosis and Treatment*; Vale, J. A., Meredith, T. J., Eds.; Update Books: London, 1981; pp 171−175. (e) Baltrop, D. In *Poisoning, Diagnosis and Treatment*; Vale, J. A., Meredith, T. J., Eds.; Update Books: London, 1981; pp 178−185.

(7) (a) Da Costa, C. P.; Rigel, H. *Inorg. Chem.* **2000**, *39*, 5985–5993. (b) Martin, R. B. *Inorg. Chim. Acta* **1998**, *283*, 30–36. (c) Magyar, J. S.; Weng, T.-C.; Stern, Ch. M.; Dye, D. F.; W. Rous, B.; Payne, J. C.; Bridgewater, M. A.; Mijovilovich, B.; Parkin, G.; Zaleski, J. M.; Penner-Hahn, J. E.; Godwin, H. A. *J. Am. Chem. Soc.* **2005**, *127*, 9495–9505.

(8) (a) Lanphear, B. P.; Hornung, R.; Khoury, J.; Yolton, K.; Baghurst, P.; Bellinger, D. C.; Canfield, R. L.; Dietrich, K. N.; Bornschein, R.; Greene, T.; Rothenberg, S. J.; Needleman, H. L.; Schnaas, L.; Wasserman, G.; Graziano, J.; Roberts, R. *Environ. Health Perspect.* **2005**, *113*, 894–899.(b) Castellino, C.; Caselino, P.; Sannolo, N. In *Inorganic Lead Exposure: Metabolism and Intoxication*; Lewis: Boca Raton, FL, 1994.

(9) Seaton, C. L.; Lasman, J.; Smith, D. R. *Toxicol. Appl. Pharmacol.* **1999**, *159*, 153–160.

(10) Sillanpaa, M.; Oikari, A. *Chemosphere* **1996**, *32*, 1485–1497.

(11) Liao, Y.; Zhang, J.; Jin, Y.; Lu, C.; Li, G.; Yu, F.; Zhi, X.; An, L.; Yang, J. *Biometals* **2008**, *21*, 1–8.
(12) Li, W. B.; Hollriegl, V.; Roth, P.; Oeh, U. *Radiat. Environ. Biophys.* **2006**, *45*, 115–124.
(13) Balonov, M. I.; Anspaugh, L. R.; Bouville, A.; Likhtarev, I. A. *Radiat. Prot. Dosim.* **2007**, *127*, 491–496.
(14) Spiers, F. W.; Vaughan, J. *Leuk. Res.* **1989**, *13*, 347–50.
(15) (a) Llobet, J. M.; Colomina, M. T.; Domingo, J. L.; Corbella, J. *Vet. Hum. Toxicol.* **1992**, *34*, 7–9. (b) Ortega, A.; Gomez, M.; Domingo, J. L.; Corbella, J. *Arch. Environ. Contam. Toxicol.* **1989**, *18*, 612–616.
(16) Sonawane, V. R.; Jagtap, V. S.; Pahuja, D. N.; Rajan, M. G. R.; Samuel, A. M. *Health Phys.* **2004**, *87*, 46–50.
(17) (a) Dietrich, B.; Lehn, J.-M.; Sauvage, J. P. *Tetrahedron Lett.* **1969**, 2889–2892. (b) Muller, W. H. *Naturwissenschaften* **1970**, *57*, 248.
(18) Gokel, G. W.; Korzeniowski, S. H. In *Macrocyclic Polyether Synthesis*; Springer: Berlin, 1982.
(19) Nakatsuji, Y.; Nakamura, T.; Yometani, M.; Yuya, H.; Okahara, M. *J. Am. Chem. Soc.* **1988**, *110*, 531–538.
(20) Chang, C. A.; Rowland, M. E. *Inorg. Chem.* **1983**, *22*, 3866–3869.
(21) Brücher, E.; Gyori, B.; Emri, J.; Jakab, S.; Kovacs, Z.; Solymosi, P.; Toth, I. *J. Chem. Soc., Dalton Trans.* **1995**, 3353–3357.
(22) Yost, T. L.; Fagan, B. C.; Allain, L. R.; Barnes, C. E.; Dai, S.; Sepaniak, M. J.; Xue, Z. *Anal. Chem.* **2000**, *72*, 5516–5519.
(23) Ferreirós-Martínez, R.; Esteban-Gómez, D.; de Blas, A.; Platas-Iglesias, C.; Rodríguez-Blas, T. *Inorg. Chem.* **2009**, *48*, 11821–11831.
(24) Ferreirós-Martínez, R.; Platas-Iglesias, C.; de Blas, A.; Esteban-Gómez, D.; Rodríguez-Blas, T. *Eur. J. Inorg. Chem.* **2010**, 2495–2503.
(25) Roca-Sabio, A.; Mato-Iglesias, M.; Esteban-Gómez, D.; Tóth, E.; de Blas, A.; Platas-Iglesias, C.; Rodríguez-Blas, T. *J. Am. Chem. Soc.* **2009**, *131*, 3331–3341.
(26) (a) Palinkas, Z.; Roca-Sabio, A.; Mato-Iglesias, M.; Esteban-Gomez, D.; Platas-Iglesias, C.; de Blas, A.; Rodriguez-Blas, T.; Toth, E. *Inorg. Chem.* **2009**, *48*, 8878–8889. (b) Mato-Iglesias, M.; Roca-Sabio, A.; Palinkas, Z.; Esteban-Gomez, D.; Platas-Iglesias, C.; Toth, E.; de Blas, A.; Rodriguez-Blas, T. *Inorg. Chem.* **2008**, *47*, 7840–7851.
(27) (a) Lacoste, R. G.; Christoffers, G. V.; Martell, A. E. *J. Am. Chem. Soc.* **1965**, *87*, 2385–2388.(b) Martell, A. E.; Motekaitis, R. J.; Smith, R. M. *NIST Critically selected stability constants of metal complexes database*, Version 8.0 for windows; National Institute of Standards and Technology: Gaithersburg, MD, 2004; Standard Reference Data Program.
(28) Chatterton, N.; Gateau, C.; Mazzanti, M.; Pécaut, J.; Borel, A.; Helm, L.; Merbach, A. E. *Dalton Trans.* **2005**, 1129–1135.
(29) (a) Mato-Iglesias, M.; Balogh, E.; Platas-Iglesias, C.; Tóth, E.; de Blas, A.; Rodríguez-Blas, T. *Dalton Trans.* **2006**, 5404–5415. (b) Ferreiros-Martinez, R.; Esteban-Gomez, D.; Platas-Iglesias, C.; de Blas, A.; Rodriguez-Blas, T. *Inorg. Chem.* **2009**, *48*, 10976–10987.
(30) Costa, J.; Delgado, R.; Drew, M. G. B.; Félix, V. *J. Chem. Soc., Daton Trans.* **1999**, 4331–4339.
(31) Vaiana, L.; Platas-Iglesias, C.; Esteban-Gómez, D.; Avecilla, F.; de Blas, A.; Rodríguez-Blas, T. *Eur. J. Inorg. Chem.* **2007**, 1874–1783.
(32) (a) Hunter, C. A.; Sanders, J. K. M. *J. Am. Chem. Soc.* **1990**, *112*, 5525–5534. (b) Song, R.-F.; Xie, Y.-B.; Li, J.-R.; Bu, X.-H. *J. Chem. Soc., Dalton Trans.* **2003**, 4742–4748.
(33) Addison, W.; Nageswara-Rao, W.; Reedijk, J.; van Rijn, J.; Verschoor, G. C. *J. Chem. Soc., Dalton Trans.* **1984**, 1349–1356.
(34) The parameter τ is the index of the degree of trigonality within the structural continuum between square-pyramidal and trigonal bipyramidal geometries. If A is the apical donor atom of a square-based pyramid then it should not be among the atoms which define the largest two angles at the metal center. Donor atoms B and C are associated with the greater basal angle, b, and atoms D and E with the smaller basal angle, a; $\tau = (b - a)/60$ and is therefore 0 for a square pyramid and 1 for a trigonal bipyramid.
(35) Shimoni-Livny, L.; Glusker, J. P.; Bock, C. W. *Inorg. Chem.* **1998**, *37*, 1853–1867.
(36) (a) Esteban-Gómez, D.; Platas-Iglesias, C.; Enríquez-Pérez, T.; Avecilla, F.; de Blas, A.; Rodríguez-Blas, T. *Inorg. Chem.* **2006**, *45*, 5407–5416. (b) Platas-Iglesias, C.; Esteban-Gómez, D.; Enriquez-Perez, T.; Avecilla, F.; de Blas, A.; Rodríguez-Blas, T. *Inorg. Chem.* **2005**, *44*, 2224–2233.
(37) (a) Cockrell, G. M.; Zhang, G.; Van der Veer, D. G.; Thummel, R. P.; Hancock, R. D. *J. Am. Chem. Soc.* **2008**, *130*, 1420–1430. (b) Gephart, R. T., III; Williams, N. J.; Reibenspies, J. H.; De Sousa, A. S.; Hancock, R. D. *Inorg. Chem.* **2008**, *47*, 10342–10348.
(38) (a) Sazonov, P. K.; Minacheva, L. K.; Churakov, A. V.; Sergienko, V. S.; Artamkina, G. A.; Oprunenko, Y. F.; Beletskaya, I. P. *Dalton Trans.* **2009**, 843–850. (b) Esteban-Gomez, D.; Ferreiros, R.; Fernandez-Martinez, S.; Avecilla, F.; Platas-Iglesias, C.; de Blas, A.; Rodriguez-Blas, T. *Inorg. Chem.* **2005**, *44*, 5428–5436. (c) Esteban, D.; Avecilla, F.; Platas-Iglesias, C.; Mahia, J.; de Blas, A.; Rodriguez-Blas, T. *Inorg. Chem.* **2002**, *41*, 4337–4347. (d) Arya, P.; Channa, A.; Cragg, P. J.; Prince, P. D.; Steed, J. W. *New J. Chem.* **2002**, *26*, 440–447. (e) Hambley, T. W.; Lindoy, L. F.; Reimers, J. R.; Turner, P.; Wei, G.; Widmer-Cooper, A. N. *J. Chem. Soc., Dalton Trans.* **2001**, 614–620.
(39) Corey, E. J.; Bailar, J. C., Jr. *J. Am. Chem. Soc.* **1959**, *81*, 2620–2629.
(40) Beattie, J. K. *Acc. Chem. Res.* **1971**, *4*, 253–259.
(41) Piguet, C.; Bünzli, J.-C. G.; Bernardinelli, G.; Bochet, C. G.; Froidevaux, P. *J. Chem. Soc., Dalton Trans.* **1995**, 83–97.
(42) Harris, R. K. In *Nuclear Magnetic Resonance Spectroscopy: A Physicochemical view*; Pitman: London, 1983.
(43) Aime, S.; Botta, M.; Ermondi, G. *Inorg. Chem.* **1992**, *31*, 4291–4299.
(44) (a) Karplus, M. *J. Am. Chem. Soc.* **1963**, *85*, 2870–2871. (b) Geraldes, C. F. G. C.; Sherry, A. D.; Kiefer, G. E. *J. Magn. Reson.* **1992**, *97*, 290–304.
(45) Shannon, R. D. *Acta Crystallogr.* **1976**, *A32*, 751–767.
(46) Hancock, R. D.; Maumela, H.; de Sousa, A. S. *Coord. Chem. Rev.* **1996**, *148*, 315–347.
(47) Adam, K. R.; Dancey, K. P.; Leong, A. J.; Lindoy, L. F.; McCool, B. J.; McPartlin, M.; Tasker, P. A. *J. Am. Chem. Soc.* **1988**, *110*, 8471–8477.
(48) Wolsey, W. C. *J. Chem. Educ.* **1973**, *50*, A335–A337.
(49) Gans, P.; Sabatini, A.; Vacca, A. *Talanta* **1996**, *43*, 1739–1753.
(50) *SABADS*, Version 2004/1; Bruker-AXS: Madison, WI.
(51) *SHELX*; Sheldrick, G. M. *Acta Crystallogr.* **2008**, *A64*, 112−122.
(52) *WinGX*, MS-Windows system of programs for solving, refining and analysing single crystal X-ray diffraction data for small molecules; Farrugia, L. F. *J. Appl. Crystallogr.* **1999**, *32*, 837–838.
(53) Beurskens, P. T.; Beurskens, G.; Gelder, R.; Smits, J. M. M.; Garcia-Granda, S.; Gould, R. O. *DIRDIF-2008 - A Computer Program for Crystal Structure Determination by Patterson Methods and Direct Methods applied to Difference Structure Factors*; Crystallography Laboratory, Radbound University Nijmegen: Nijmegen, The Netherlands, 2008.
(54) Nardelli, M. *Appl. Crystallogr.* **1999**, *32*, 563–571.
(55) Becke, A. D. *J. Chem. Phys.* **1993**, *98*, 5648–5652.
(56) Lee, C.; Yang, W.; Parr, R. G. *Phys. Rev. B* **1988**, *37*, 785–789.
(57) Frisch, M. J.; Trucks, G. W.; Schlegel, H. B.; Scuseria, G. E.; Robb, M. A.; Cheeseman, J. R.; Montgomery, Jr., J. A.; Vreven, T.; Kudin, K. N.; Burant, J. C.; Millam, J. M.; Iyengar, S. S.; Tomasi, J.; Barone, V.; Mennucci, B.; Cossi, M.; Scalmani, G.; Rega, N.; Petersson, G. A.; Nakatsuji, H.; Hada, M.; Ehara, M.; Toyota, K.; Fukuda, R.; Hasegawa, J.; Ishida, M.; Nakajima, T.; Honda, Y.; Kitao, O.; Nakai, H.; Klene, M.; Li, X.; Knox, J. E.; Hratchian, H. P.; Cross, J. B.; Adamo, C.; Jaramillo, J.; Gomperts, R.; Stratmann, R. E.; Yazyev, O.; Austin, A. J.; Cammi, R.; Pomelli, C.; Ochterski, J. W.; Ayala, P. Y.; Morokuma, K.; Voth, G. A.; Salvador, P.; Dannenberg, J. J.; Zakrzewski, V. G.; Dapprich, S.; Daniels, A. D.; Strain, M. C.; Farkas, O.; Malick, D. K.; Rabuck, A. D.; Raghavachari, K.; Foresman, J. B.; Ortiz, J. V.; Cui, Q.; Baboul, A. G.; Clifford, S.; Cioslowski, J.; Stefanov, B. B.; Liu, G.; Liashenko, A.; Piskorz, P.; Komaromi, I.; Martin, R. L.; Fox, D. J.; Keith, T.; Al-Laham, M. A.; Peng, C. Y.; Nanayakkara, A.; Challacombe, M.; Gill, P. M. W.; Johnson, B.; Chen, W.; Wong, M. W.; Gonzalez, C.; Pople, J. A. *Gaussian 03*, Revision C.01; Gaussian, Inc.: Wallingford, CT, 2004.

(58) (a) Hay, P. J.; Wadt, W. R. *J. Chem. Phys.* **1985**, *82*, 270–283. (b) Hay, P. J.; Wadt, W. R. *J. Chem. Phys.* **1985**, *82*, 284–298. (c) Hay, P. J.; Wadt, W. R. *J. Chem. Phys.* **1985**, *82*, 299–310.
(59) Barone, V.; Cossi, M. *J. Phys. Chem. A* **1998**, *102*, 1995–2001.
(60) Glendening, E. D.; Reed, A. E.; Carpenter, J. E.; Weinhold, F. *NBO*, version 3.1.
(61) Reed, A. E.; Curtiss, L. A.; Weinhold, F. *Chem. Rev.* **1988**, *88*, 899–926.